2014

Tactile Imaging of an Imbedded Palpable Structure for Breast Cancer Screening

Chieu Van Nguyen
University of Nebraska-Lincoln

Ravi F. Saraf
University of Nebraska-Lincoln, rsaraf2@unl.edu

# Tactile Imaging of an Imbedded Palpable Structure for Breast Cancer Screening

Chieu Van Nguyen[†] and Ravi F. Saraf[*,†,‡]

[†]Department of Chemical and Biomolecular Engineering, [‡]Nebraska Center for Materials and Nanoscience, University of Nebraska—Lincoln, Lincoln, Nebraska 68588, United States

S *Supporting Information*

ABSTRACT: Apart from texture, the human finger can sense palpation. The detection of an imbedded structure is a fine balance between the relative stiffness of the matrix, the object, and the device. If the device is too soft, its high responsiveness will limit the depth to which the imbedded structure can be detected. The sensation of palpation is an effective procedure for a physician to examine irregularities. In a clinical breast examination (CBE), by pressing over 1 cm^2 area, at a contact pressure in the 70−90 kPa range, the physician feels cancerous lumps that are 8- to 18-fold stiffer than surrounding tissue. Early detection of a lump in the 5−10 mm range leads to an excellent prognosis. We describe a thin-film tactile device that emulates human touch to quantify CBE by imaging the size and shape of 5−10 mm objects at 20 mm depth in a breast model using ~80 kPa pressure. The linear response of the device allows quantification where the greyscale corresponds to the relative local stiffness. The (background) signal from <2.5-fold stiffer objects at a size below 2 mm is minimal.

KEYWORDS: tactile sensor, palpability, breast cancer screening, nanoparticle, nanoelectronics
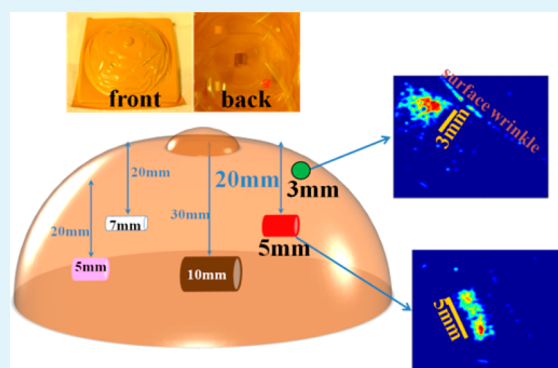
INTRODUCTION

With an estimate of almost 300 000 new cases diagnosed in 2013, accounting for 29% of all cancers, breast cancer is the most common type of cancer among women.[1] Similar to other types of cancers, an abnormal mass (or a lump) develops in the breast and is either benign (in situ) or cancerous (invasive). Growing in size with time, it eventually spreads out to neighboring regions. While there is no cure today, early diagnosis when the lump is less than 10 mm can improve the survival rate to more than 94%.[1] Using X-ray radiation, mammography images the lump based on (<50%) density contrast between the lump and surrounding tissue, which is not an effective approach for young women or women with dense and vascular breasts.[2] Medical imaging tools, such as magnetic resonance imaging (MRI) and ultrasound, are more sensitive than mammography but are too expensive to use as a screening tool. Palpability is a more effective parameter to detect malignancy, especially in younger women.[3] The higher the palpability of the lump, the greater the probability it is malignant irrespective of size.[4] Typically, the malignant lump is 8- to 18-fold stiffer than surrounding tissue.[5] Clinical breast examination (CBE) is the recommended complementary tool to mammography as it measures palpability.[6] CBE is an inexpensive, radiation-free procedure that can be performed in an out-patient setting where a professional manually feels the patient's breasts for lumps.[7] However, the result is qualitative

with no tangible recordkeeping,[7] and the typical size of lump detected is above 21 mm.[8]

The rapid development of thin-film tactile devices in recent years, also called "electronic skin," has been spurred by a variety of applications, such as robotics, minimally invasive surgery, haptics, and prosthetics,[9−12] which all have a natural extension to quantitatively image palpability by touch.[13] The contact pressure corresponding to the texture and/or shape of the object is mapped by measuring the local deformation of the tactile-device film to form a continuous or pixelated image. Typically, the local deformation is measured by probing the modulation in conductivity of a granular composite,[14−16] capacitance,[17−19] piezoresistance,[14,15,20,21] or refractive index.[22,23] Sensitivity to touch of less than 1 Pa has been demonstrated.[24] Resolution of 20 μm has been achieved for a contact area of 1 cm^2.[25] A variety of materials have been utilized to fabricate the tactile device based on the above principle, such as nanoparticles (NPs),[25−27] carbon nanotubes,[28] and nanowires.[29−32] To image palpable features in the breast, a key requirement is the emulation of human touch with optimum sensitivity in a pressure range of 50−90 kPa over a contact area in excess of 1 cm^2. Higher sensitivity would saturate the image, preventing visualization of a deeper imbedded mass. Lower
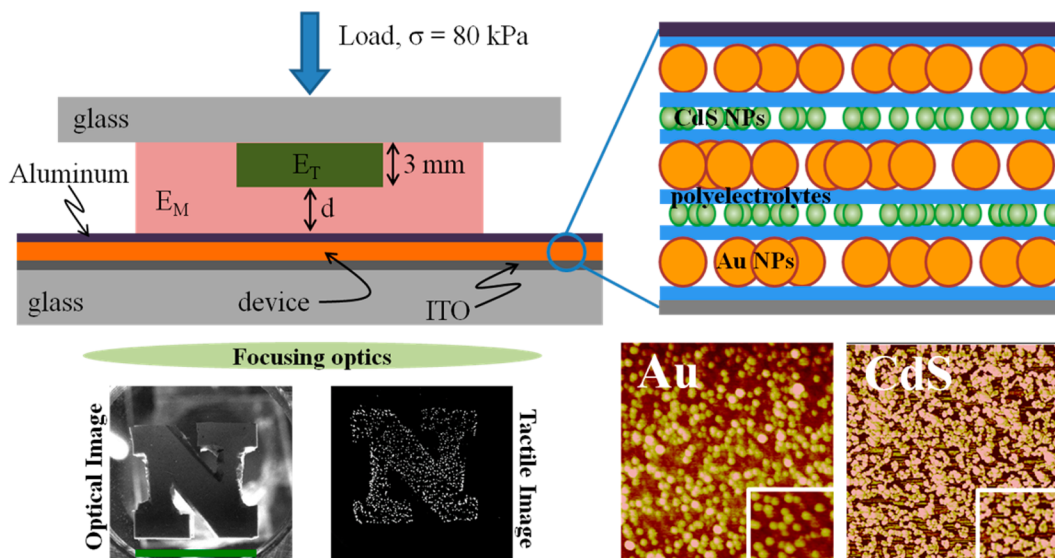
Figure 1. Schematic of touch experiment. A touch pressure applied on the top through a glass slide compressed the palpable structure on the tactile device. A constant bias of 18 V was supplied across the top (Al) and bottom electrodes (ITO). An N-shaped object was imaged via touch experiment with d = 3 mm, E_T/E_M = 10. The green bar in the optical image is 12 mm. The tactile image at 80 KPa load clearly shows sharp features of <2 mm. The SPM images of Au and CdS NPs layers are 500 nm × 500 nm; the insets are 100 nm × 100 nm.
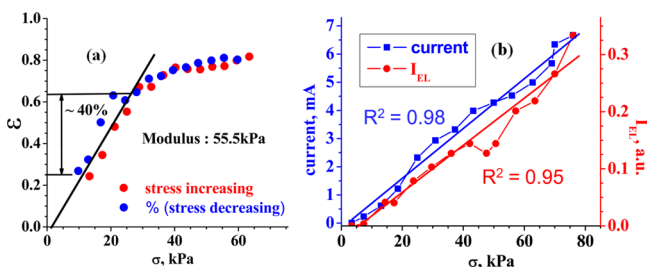
Figure 2. Mechanical properties of the thin film tactile device. Strain−stress relationship was obtained from electromechanical measurements (a). The modulus of the thin film was computed from the linear region, as indicated by the black line. Electrical current and EL were measured as functions of stress (b).

sensitivity would require a significant amount of applied pressure, leading to discomfort. Recently, several tactile devices for imaging breast cancer lumps have been reported. SureTouch, a commercial product, can image a 22-fold stiffer mass with a diameter of 6 mm and 11 mm at a depth of 17 mm and 27 mm, respectively.[13] Based on piezoresistivity,[33] piezoelectricity,[16] vibration,[34] and IR pressure sensors,[35] masses as small as 10 mm in diameter and up to 20 mm in depth with a stiffness contrast 5- to 8-fold larger than surrounding tissue have been detected.[35] However, the resolution is only in the 2.8 mm range, making the image quality poor and determining the shape of the lump difficult. The shape, especially the irregularities, is a critical feature for classification (malignancy) of breast cancer tumors[36] (see Figure S1 Supporting Information (SI)) and at the skin level to diagnose other cancers, such as melanoma.[37]

Here, we describe a tactile device to quantitatively image a 5- to 10-fold stiffer object imbedded as much as 20 mm deep in a softer matrix. The light emitted is linearly proportional to local stress. The tactile device is a multilayer composite thin film consisting of nanoparticles (NPs) and polymers. The film is an analog electro-optical device where the imbedded stiffness is imaged as continuous variation in light emission that can be

focused directly on a camera. The electro-mechanical characteristics of the flexible thin film are precisely tuned to obtain a tactile image of the palpable structure for contact pressure in the 30 to 90 kPa range, similar to human touch. About 5 mm stiff features embedded 20 mm deep in an artificial breast model are imaged to demonstrate the performance of the device. Features softer than 2.5-fold relative to the surrounding material do not produce a significant background. The image has sufficient resolution to determine both the size and shape of the mass.

The tactile device was fabricated by the layer-by-layer spin coating of two polyelectrolytes, poly(allylamine hydrochloride) (PAH) and poly(styrenesulfonate) (PSS), and the deposition of 10 nm Au and 3 nm CdS NPs.[38] The overall multilayer structure was a total of three and two layers of Au and CdS NPs deposited alternatively and separated by nine layers of PAH and PSS (Figure 1). The device was deposited on a 25 × 25 mm^2 ITO glass substrate. The active area of the device was 500 mm^2. The ITO served as the bottom electrode. The top electrode was a smooth aluminum foil. The top surface of the device was protected with an additional PAH−PSS bilayer. The overall thickness of the thin film device was ∼150 nm. A Scanning Probe Microscope (SPM) image of each layer shows that the deposition is well below the in-plane percolation threshold; i.e., the device is not conductive along the film direction (Figure 1). Well over 30 devices are fabricated and tested to confirm the principle and the performance. The samples subjected to load for imaging are robust and unchanged well over 100 experiments, and stable over 6 months stored in air in an unsealed container.

To quantitatively study the performance of the device for imaging palpability, a composite structure was fabricated with a soft silicone foam matrix of modulus E_M ∼ 178 kPa imbedded with a stiffer filler (of fixed thickness, 3 mm; see Figure S2 in SI). The filler was a combination of silicone sponge (E_T ∼ 415 kPa) and two types of silicone rubbers (E_T ∼ 879 and 1744 kPa). The details of the materials are included in the Methods section. Depending on the filler materials, the stiffness ratio,
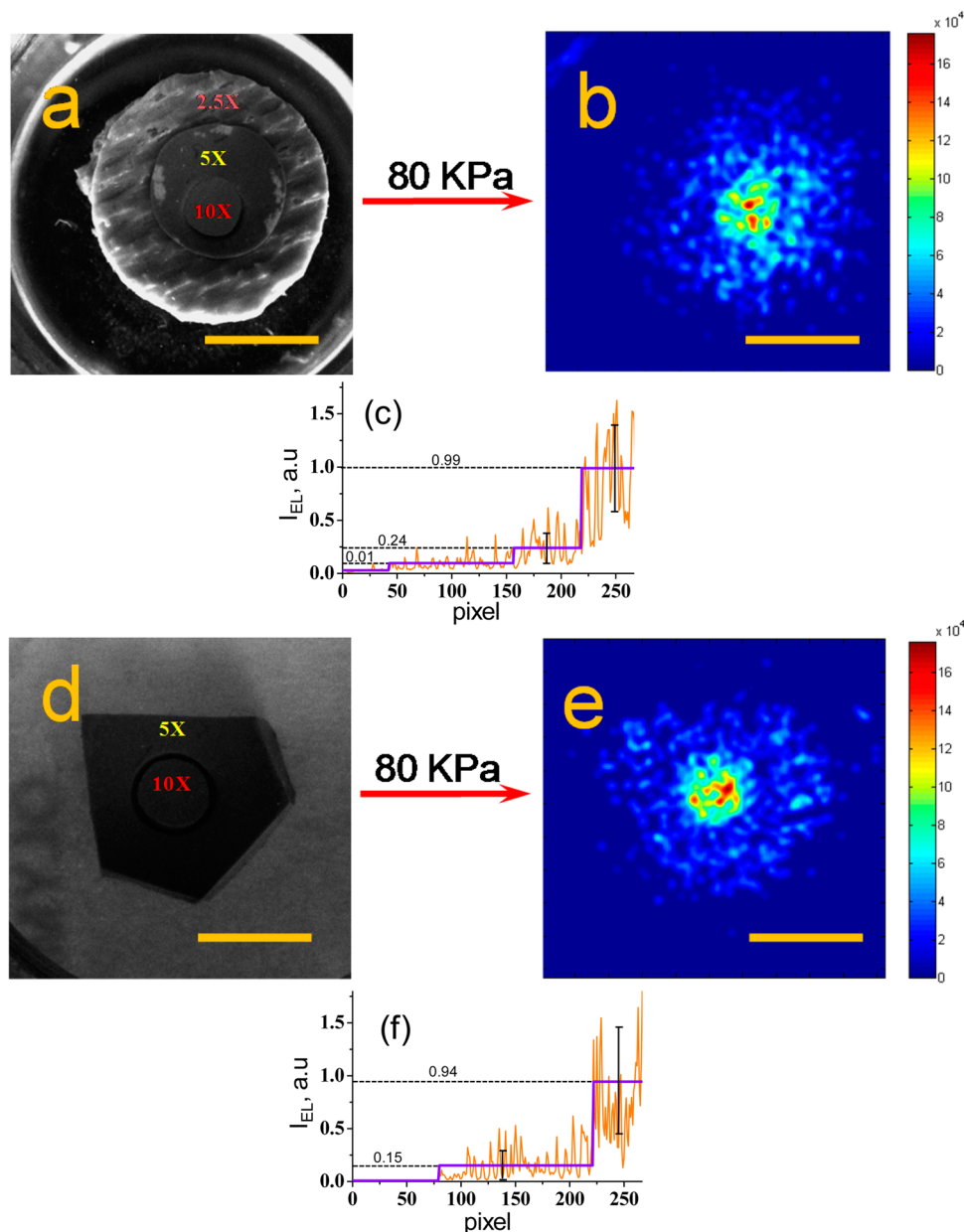
Figure 3. Tactile images of heterogeneous palpable structures. (a) Optical image of cocentric filler with E_T/E_M ranging from 10 to 2.5 in the radial direction. (b and c) Corresponding tactile image and a typical line scan. (d) Optical image of jagged and circular-shaped filler with E_T/E_M = 5, 10, respectively. (e and f) Corresponding tactile image and a typical line scan. The horizontal purple line in c and f is average I_{EL}. The error bars in c are 0.14 and 0.4; in f, they are are 0.13 and 0.5, respectively. The scale bar is 5 mm. The I_{EL} is in arbitrary units.

E_T/E_M, ranged from 2.5 to 10. In a typical imaging experiment, the composite structure was placed above the device, and a constant load of 80 kPa was applied (Figure 1). The lateral dimension of the filler, L, and the depth from the contact, d, were varied (as described later). On pressing against the tactile device, the pressure distribution was uneven, corresponding to modulation in the local stiffness relative to the surrounding matrix. The device was like an electro-optical "strain gauge" that converts the compressive stress to electroluminescence intensity (I_{EL}) from the CdS nanoparticles.[40] Under the applied bias of 18 V, the potential gradient (drop) across the CdS NPs layers is greater than its bandgap (~2.4 eV), large enough to form an electron−hole pair, resulting in electroluminescence. The tactile image was obtained by focusing the

distribution of emitted I_{EL} on a CCD camera (Roper Cascade II).

The principle of the device is similar to compression-sensitive elastomer used in electronic skin, except the thickness is only ~150 nm with a reversible stress−strain response of over 40% compression and linearity up to 60% (Figure 2a). The mechanical properties of the tactile device are obtained by applying uniform compressive stress, σ, on the film at a constant bias and measuring the change in resistance to calculate the strain as $\varepsilon = (R_O^{0.5} − R^{0.5})/R_O^{0.5}$, where R_O is the resistance at $\varepsilon = 0$.[38] The $\sigma − \varepsilon$ characteristics indicate that the device film deforms linearly at a modulus of 55.5 kPa (Figure 2a). The low modulus and high compressibility of the device are attributed to local (reversible) buckling of the polymer interpose layer.[38] The low modulus at 55.5 kPa allows the
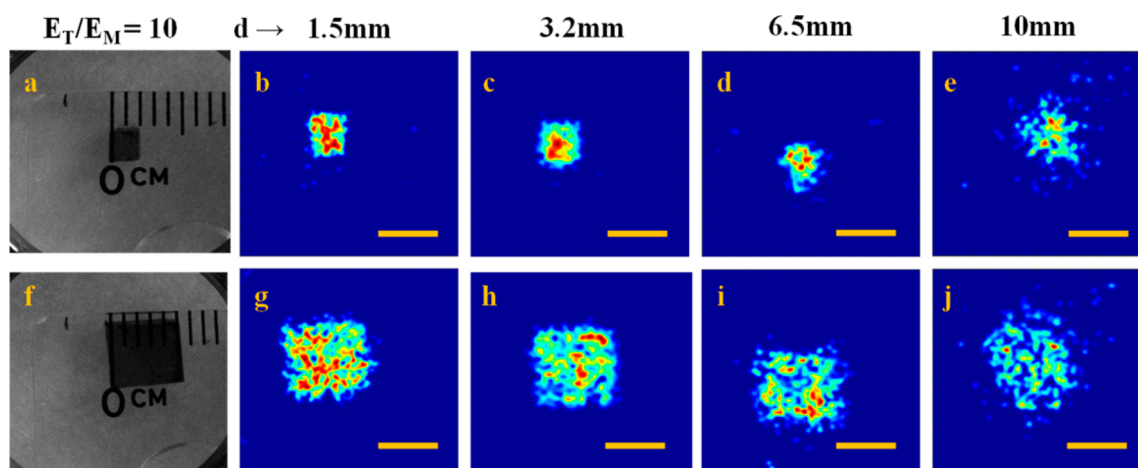
Figure 4. Effect of the d on the tactile image. (a and f) Optical image of filler with square cross-section of side 2 and 5 mm, respectively. The other panels (b to e and g to j) are corresponding tactile images at d ranging from 1.5 to 10 mm. The stiffness ratio, E_T/E_M, is fixed at 10. Scale bar is 5 mm.
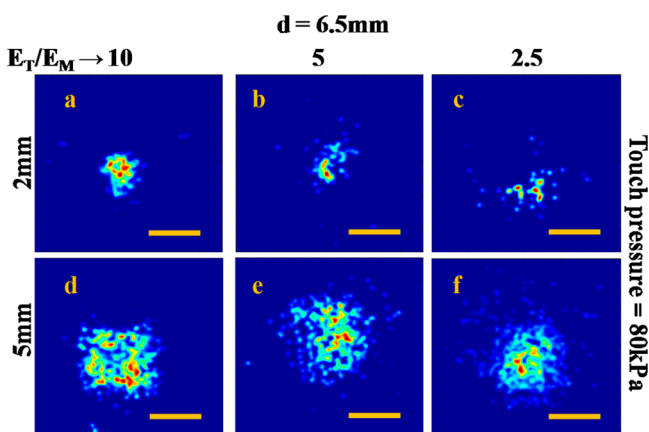
Figure 5. Study of the effect of E_T/E_M on the tactile image. (a to f) Using the same filler shape as Figure 4. Tactile images at E_T/E_M ranging from 2.5 to 10 are recorded. The filler is fixed at $d = 6.5$ mm. Color scale is similar to that of Figure 2. Scale bar is 5 mm.

tunability for tactile imaging at 80 kPa that is comparable to human touch. The device is highly linear in terms of both the current and I_{EL} (Figure 2b). The linearity is due to the increase in the number of percolation channels per unit of a cross-sectional area as the film is compressed. The electroluminescence conversion is high, corresponding to low power consumption, ~0.25 mW/mm^2, comparable to other electronic skin sensors (~0.6 mW/mm^2)[40]. As I_{EL} is linearly proportional to the local strain, the greyscale of the tactile image maps the local stiffness variation.

Two classes of palpable composite structures were fabricated to quantitatively image the variation in stiffness and anisotropic shape of the filler, respectively. For both structures, the filler $d = 3.2$ mm deep. In the first structure, the cross-section was circular with E_T/E_M from 2.5 to 10 (Figure 3a). The corresponding tactile image clearly shows the gradual decrease in contrast (i.e., lower EL) as E_T/E_M decreased from 10 to 2.5 (Figure 3b). A critical aspect of the device is the ability to quantify the relative palpability. In the image (Figure 3b), the step changes in the palpability as E_T/E_M changes from 10 to 2.5 are quantified by line scan (Figure 3c). The line is a local average over the digital values for all the pixels in that segment, and the error bar is the standard deviation. Although the

standard deviations are large, there appears to be a clear distinction between the three (local) hardness regions. The relative increases in average EL from 2.5 to 5 and 5 to 10 was ~2.4 and ~4.1, respectively, which are reasonably linear. The strong contrast in the tactile image for E_T/E_M above 5 meets the breast cancer screening requirement of imaging a mass of stiffness 10-fold higher than surrounding tissue.[5] The second composite structure had two fillers, but the cross-section was noncircular with sharp corners (Figure 3d). The image clearly shows the noncircular-shaped "corona" for E_T/E_M of 5 and the circular-shaped central core with larger intensity. In a similar analysis to that for Figure 3c, the linear scan across the image shows a rise in intensity of ~6-fold (Figure 3f).

We quantified the effect of d at fixed E_T/E_M and, conversely, the effect of E_T/E_M at fixed d, on the image quality. The fillers were 3 mm thick (see Figure 1) with an $L = 2$ mm and 5 mm square cross-section, respectively (Figure 4a,f). The $E_T/E_M = 10$ was fixed. For shallow depths, $d \leq 3.2$ mm, the contrast was remarkable with sharp edges and corners (Figure 4). The 2 mm mass (i.e., filler) was easily detected up to depths of 10 mm. However, the sharp edges at $d = 10$ mm were smeared. The circular-like shape and larger apparent size at a 10 mm depth was because the differential stress field due to the filler tends to become isotropic. For larger sizes, the shape appeared to be intact. Importantly, for $E_T/E_M = 10$, the required minimum stiffness ratio to detect cancerous tumors in the breast and palpable filler of $L = 2$ mm at $d = 10$ mm is clearly visible in the tactile images. The EL intensity in all tactile images was color-coded with a scale similar to that shown in Figure 2. The sharp images with defined corners are consistent with the high resolution of ~20 μm measured for the tactile device.[25] The high resolution is attributed to the anisotropic conduction of the film where electron tunneling occurs along the thickness but the interparticle spacing in the lateral direction is sparse for percolation (Figure 1). As a result, in principle, the effective pixel size (accounting for incommensurability between the layers) is below 100 nm.

Next, $d = 6.5$ mm was fixed, and the effect of E_T/E_M was studied. The fillers were identical, as in Figure 4. Tactile images for $L = 2$ mm filler were detectable for $E_T/E_M = 10$ (Figure 5a). For $E_T/E_M = 5$, the shape was not apparent, while at 2.5, the filler was below the detection limit. It is important to note that
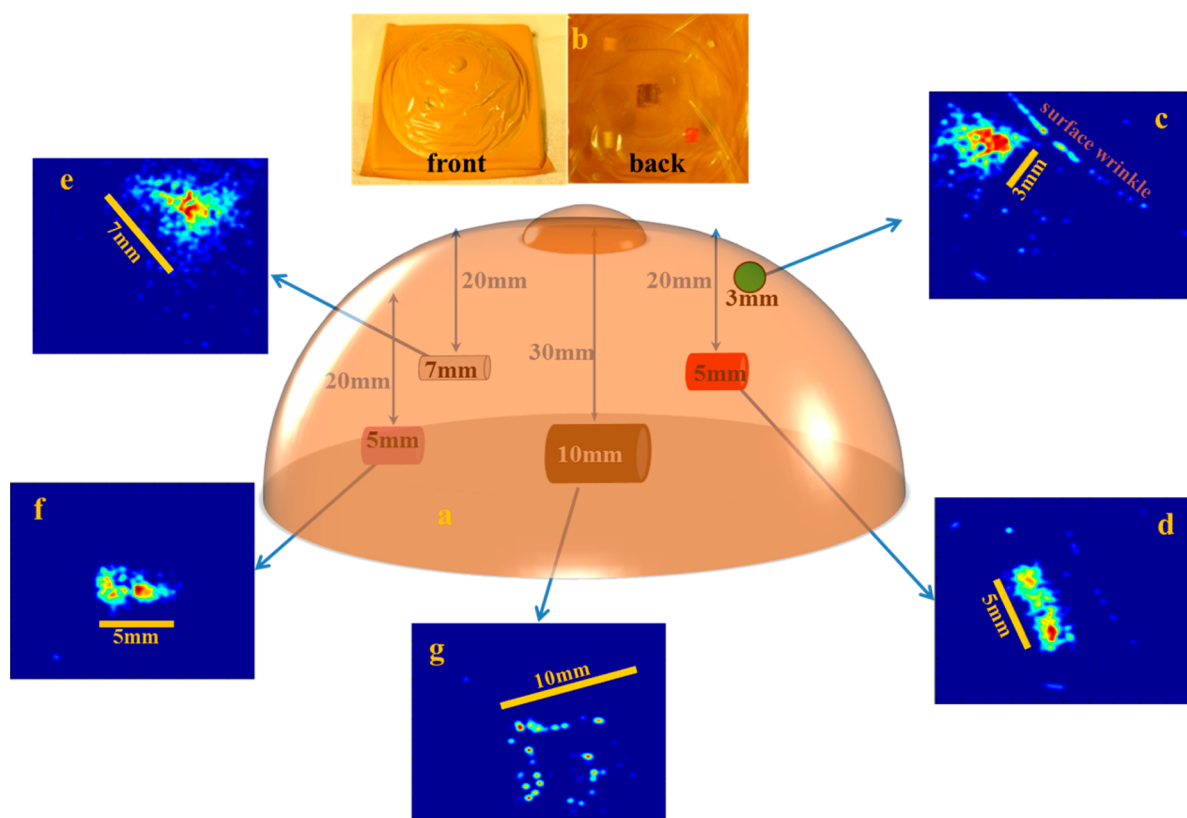
Figure 6. Tactile imaging of a breast model. (a and b) Schematic and optical image of the breast model, respectively. (c to g) Tactile images of the various fillers in the model. The wrinkles in the model surface (b) are visible in the tactile images (for example, c and d).

for this particular depth and $E_T/E_M < 5$, the 2 mm filler was undetectable by human fingers. The larger filler ($L = 5$ mm), however, was clearly visible in the images for all E_T/E_M values. The device can clearly image fillers larger than 5 mm even at low stiffness ratio. This suggests that a small variation in the stiffness (below 2.5) of a size less than 2 mm, which may be due to (normal) heterogeneity in the breast tissue, will not be visible, indicating a low background and leading to higher contrast in tactile images for features with higher relative stiffness.

A translucent breast model with visible fillers of relative stiffness of $E_T/E_M = 10$ from MammaCare Corp. was tested (Figure 6a). The mechanical properties of the breast model are realistic in terms of overall stiffness and are used to train medical personnel for CBE. The fillers of different shapes and size are located at depths ranging from ~2 to 20 mm (Figure 6b). The tactile image of each of the fillers (i.e., simulated mass) 20 mm below the surface were correctly detected in the tactile images, including the anisotropic shape (Figure 6c−f). Dimensions of 5 mm are clearly apparent (Figure 6d), indicating that the device can potentially be a screening tool to emulate CBE. Similar to a mass in the breast, the filler in the breast model is mobile in the surrounding matrix during palpation. The movement is recorded as distortion of the image as the angle of palpation is changed (Figures S3 and S4 in SI). It is also of note that small distortion occurs because during the palpation the filler is mobile, so only a portion of the filler produces the stress distribution. Unfortunately, the filler under the papilla could not be imaged properly although it was the largest (Figure 6g). However, the outline of the image is visible

but not too conclusive. Feeling a mass under the papilla also remains a challenge for CBE.

CONCLUSION

In summary, the device has four salient features that allow for optimum sensitivity to obtain palpable images 20 mm deep of a 5 mm size structure. First, although the film was only ~150 nm, it was sensitive to appreciable strain caused by contact pressure in the 80 kPa range. The local buckling of the polymer film between the nanoparticle layers resulted in counterintuitive softening of the film and reversible deformation of up to a 40% compression ratio (Figure 2b). The second aspect of the device is the linear response. The optical signal and the rise in electrical current on compression increased linearly with load (Figure 2a). The linearity was caused by a linear increase in the percolation path between the top and bottom electrode with increasing load. The tunneling current did rise due to compression, but the effect was insignificant compared to the increase in percolation. The third aspect was easy processing by a simple dip coating and washing operation that allowed fabrication of the device on a large area flat or curved surface and substrates that may be rigid or flexible. The fourth aspect was that the signal from the film was continuous (i.e., an analog device) where the contact pressure was directly converted to EL distribution making the data acquisition convenient and fast. Using an artificial breast model, the four features resulted in imaging palpability of clinical relevance to potentially screen for breast cancer. The smallest mass imaged by devices reported in the literature was 6 mm in diameter at a depth of up to 17.5 mm, but the stiffness ratio was ~22.[13] In a breast model, a 5 mm long mass was accurately imaged at a depth of 20 mm (3

times the thickness of the mass itself) and E_T/E_M was as low as 10. Masses smaller than 10 mm in length were often difficult to detect even by a trained professional.[8] Thus, the device will improve the outcome of CBE by providing a quantitative image. Softer masses ($E_T/E_M < 2.5$) were below the sensitivity level leading to background. Owing to the linear response of the device, the greyscale quantitatively mapped the relative palpability.

■ METHODS

The tactile sensor is fabricated by interposing three monolayers of Au (10 nm) and two monolayers of CdS (3 nm) spaced by dielectric polymer film (DPF). The DPF is made by spin coating alternate layers of PAH and PSS at 3000 rpm for 20 s and washing with DI H_2O also at 3000 rpm in 20 s after each deposition. Thus, the tactile sensor has the following tandem structure: ITO−DPF−(Au−DPF−CdS−DPF)$_2$−Au−DPF. The top layer is DPF for protective purposes. The structure and process is described in more detail in the literature.[38] The device is deposited on 25×25 mm^2 ITO glass (Delta Technologies Limited, CB-90IN-0105). PAH (15 000 Da) and PSS (70 000 Da) were purchased from Sigma-Aldrich.

The palpable structures are designed in a matrix of extrasoft cellular silicone (Rogers Corporation, BF-1000 in 1.5 mm, 3.2 mm, and 6.5 mm thicknesses). The filler was a closed cell silicone sponge (Rogers Corporation) and/or a silicone rubber sheet (McMaster-Carr, 8632K44). The sponge is 2.5- and 5-fold stiffer than the matrix, and the silicone rubber is 10-fold stiffer than the matrix. Their mechanical properties are investigated with a tensile test instrument (TestResources; Model 225LB Actuator and Model 3397-136 Load Cell). The results on mechanical properties are shown in Figure S2 in the SI.

■ ASSOCIATED CONTENT

Ⓢ Supporting Information

Mechanical properties of the silicone materials used in palpable touch experiments and two sets of tactile images of two breast masses. This material is available free of charge via the Internet at http://pubs.acs.org.

■ AUTHOR INFORMATION

Corresponding Author

*E-mail: rsaraf2@unl.edu.

Notes

The authors declare no competing financial interest.

■ ACKNOWLEDGMENTS

■ REFERENCES

(1) Siegel, R.; Ma, J. M.; Zou, Z. H.; Jemal, A. Cancer Statistics, 2014. *Ca-Cancer J. Clin.* **2014**, *64*, 9−29.

(2) Carney, P. A.; Miglioretti, D. L.; Yankaskas, B. C.; Kerlikowske, K.; Rosenberg, R.; Rutter, C. M.; Geller, B. M.; Abraham, L. A.; Taplin, S. H.; Dignan, M.; Cutter, G.; Ballard-Barbash, R. Individual and Combined Effects of Age, Breast Density, and Hormone Replacement Therapy Use on the Accuracy of Screening Mammography. *Ann. Int. Med.* **2003**, *138*, 168−175.

(3) Hislop, T. G.; Worth, A. J.; Kan, L.; Rousseau, E. Post Screen-Detected Breast Cancer within the Screening Mammography Program of British Columbia. *Breast Cancer Res. Treat.* **1997**, *42*, 235−242.

(4) Skinner, K. A.; Silberman, H.; Sposto, R.; Silverstein, M. J. Palpable Breast Cancers are Inherently Different from Nonpalpable Breast Cancers. *Ann. Surg. Oncol.* **2001**, *8*, 705−710.

(5) Wellman P.; Howe R. D.; Dalton E.; Kern K. A. *Breast Tissue Stiffness in Compression is Correlated to Histological Diagnosis*, s.I.: Harvard BioRobotics Laboratory Technical Report: Harvard: Cambridge, MA, 1999.

(6) McDonald, S.; Saslow, D.; Alciati, M. H. Performance and Reporting of Clinical Breast Examination: A Review of the Literature. *Ca-Cancer J. Clin.* **2004**, *54*, 345−361.

(7) Saslow, D.; Hannan, J.; Osuch, J.; Alciati, M. H.; Baines, C.; Barton, M.; Bobo, J. K.; Coleman, C.; Dolan, M.; Gaumer, G.; Kopans, D.; Kutner, S.; Lane, D. S.; Lawson, H.; Meissner, H.; Moorman, C.; Pennypacker, H.; Pierce, P.; Sciandra, E.; Smith, R.; Coates, R. Clinical Breast Examination: Practical Recommendations for Optimizing Performance and Reporting. *Ca-Cancer J. Clin.* **2004**, *54*, 327−344.

(8) Guth, U.; Huang, D. J.; Huber, M.; Schotzau, A.; Wruk, D.; Holzgreve, W.; Wight, E.; Zanetti-Dallenbach, R. Tumor Size and Detection in Breast Cancer: Self-Examination and Clinical Breast Examination are at their Limit. *Cancer Detect. Prev.* **2008**, *32*, 224−228.

(9) Hammock, M. L.; Chortos, A.; Tee, B. C. K.; Tok, J. B. H.; Bao, Z. A. 25th Anniversary Article: The Evolution of Electronic Skin (E-Skin): A Brief History, Design Considerations, and Recent Progress. *Adv. Mater.* **2013**, *25*, 5997−6037.

(10) Dahiya, R. S.; Metta, G.; Valle, M.; Sandini, G. Tactile Sensing-From Humans to Humanoids. *IEEE Trans. Robot.* **2010**, *26*, 1−20.

(11) Mittendorfer, P.; Cheng, G. Humanoid Multimodal Tactile-Sensing Modules. *IEEE Trans. Robot.* **2011**, *27*, 401−410.

(12) Alvares, D.; Wieczorek, L.; Raguse, B.; Ladouceur, F.; Lovell, N. H. Development of Nanoparticle Film-Based Multi-Axial Tactile Sensors for Biomedical Applications. *Sens. Actuators, A* **2013**, *196*, 38−47.

(13) Egorov, V.; Sarvazyan, A. P. Mechanical Imaging of The Breast. *IEEE Trans. Med. Imag.* **2008**, *27*, 1275−1287.

(14) Dargahi, J.; Parameswaran, M.; Payandeh, S. A Micromachined Piezoelectric Tactile Sensor for an Endoscopic Grasper - Theory, Fabrication and Experiments. *J. Microelectromech. Syst.* **2000**, *9*, 329−335.

(15) Kolesar, E. S.; Dyson, C. S. Object Imaging with a Piezoelectric Robotic Tactile Sensor. *J. Microelectromech. Syst.* **1995**, *4*, 87−96.

(16) Yegingil H. O. *Breast Cancer Detection and Differentiation Using Piezoelectric Fingers*. Ph.D. Thesis, Drexel University, Philadelphia, PA, 2009.

(17) Cotton, D. P. J.; Graz, I. M.; Lacour, S. P. A Multifunctional Capacitive Sensor for Stretchable Electronic Skins. *IEEE Sensors J.* **2009**, *9*, 2008−2009.

(18) Metzger, C.; Fleisch, E.; Meyer, J.; Dansachmuller, M.; Graz, I.; Kaltenbrunner, M.; Keplinger, C.; Schwodiauer, R.; Bauer, S. Flexible-Foam-Based Capacitive Sensor Arrays for Object Detection at Low Cost. *Appl. Phys. Lett.* **2008**, *92*, 013506.

(19) Sato, N.; Shigematsu, S.; Morimura, H.; Yano, M.; Kudou, K.; Kamei, T.; Machida, K. Novel Surface Structure and Its Fabrication Process for MEMS Fingerprint Sensor. *IEEE Trans. Electron Devices* **2005**, *52*, 1026−1032.

(20) Smith, C. S. Piezoresistance Effect in Germanium and Silicon. *Phys. Rev.* **1954**, *94*, 42−49.

(21) Xiao, X.; Yuan, L. Y.; Zhong, J. W.; Ding, T. P.; Liu, Y.; Cai, Z. X.; Rong, Y. G.; Han, H. W.; Zhou, J.; Wang, Z. L. High-Strain Sensors Based on ZnO Nanowire/Polystyrene Hybridized Flexible Films. *Adv. Mater.* **2011**, *23*, 5440−5444.

(22) Maekawa, H.; Tanie, K.; Komoriya, K. A Finger-Shaped Tactile Sensor Using an Optical Waveguide. *Systems, Man and Cybernetics, 1993. Systems Engineering in the Service of Humans', Conference Proceedings, International Conference on*; IEEE: 1993; Vol 5, pp 403−408.

(23) Wang, A.; He, S.; Fang, X.; Jin, X.; Lin, J. Optical Fiber Pressure Sensor Based on Photoelasticity and Its Application. *J. Lightwave Technol.* **1992**, *10*, 1466−1472.

(24) Pan, L. J.; Chortos, A.; Yu, G. H.; Wang, Y. Q.; Isaacson, S.; Allen, R.; Shi, Y.; Dauskardt, R.; Bao, Z. N. An Ultra-Sensitive Resistive Pressure Sensor Based on Hollow-Sphere Microstructure Induced Elasticity in Conducting Polymer Film. *Nat. Commun.* **2014**, *5*, 3002.

(25) Maheshwari, V.; Saraf, R. F. High-Resolution Thin-Film Device to Sense Texture by Touch. *Science* **2006**, *312*, 1501−1504.

(26) Segev-Bar, M.; Haick, H. Flexible Sensors Based on Nanoparticles. *ACS Nano* **2013**, *7*, 8366−8378.

(27) Segev-Bar, M.; Landman, A.; Nir-Shapira, M.; Shuster, G.; Haick, H. Tunable Touch Sensor and Combined Sensing Platform: Toward Nanoparticle-based Electronic Skin. *ACS Appl. Mater. Interfaces* **2013**, *5*, 5531−5541.

(28) Lipomi, D. J.; Vosgueritchian, M.; Tee, B. C. K.; Hellstrom, S. L.; Lee, J. A.; Fox, C. H.; Bao, Z. N. Skin-Like Pressure and Strain Sensors Based on Transparent Elastic Films of Carbon Nanotubes. *Nat. Nanotechnol.* **2011**, *6*, 788−792.

(29) Wu, W. Z.; Wen, X. N.; Wang, Z. L. Taxel-Addressable Matrix of Vertical-Nanowire Piezotronic Transistors for Active and Adaptive Tactile Imaging. *Science* **2013**, *340*, 952−957.

(30) Pan, C. F.; Dong, L.; Zhu, G.; Niu, S. M.; Yu, R. M.; Yang, Q.; Liu, Y.; Wang, Z. L. High-Resolution Electroluminescent Imaging of Pressure Distribution Using a Piezoelectric Nanowire LED Array. *Nat. Photonics* **2013**, *7*, 752−758.

(31) Zhu, G.; Yang, W. Q.; Zhang, T. J.; Jing, Q. S.; Chen, J.; Zhou, Y. S.; Bai, P.; Wang, Z. L. Self-Powered, Ultrasensitive, Flexible Tactile Sensors Based on Contact Electrification. *Nano Lett.* **2014**, *14*, 3208−3213.

(32) Mannsfeld, S. C. B.; Tee, B. C. K.; Stoltenberg, R. M.; Chen, C. V. H.; Barman, S.; Muir, B. V. O.; Sokolov, A. N.; Reese, C.; Bao, Z. N. Highly Sensitive Flexible Pressure Sensors with Microstructured Rubber Dielectric Layers. *Nat. Mater.* **2010**, *9*, 859−864.

(33) Wellman, P. S.; Dalton, E. P.; Krag, D.; Kern, K. A.; Howe, R. D. Tactile Imaging of Breast Masses - First Clinical Report. *Arch. Surg.* **2001**, *136*, 204−208.

(34) Murayama, Y.; Haruta, M.; Hatakeyama, Y.; Shiina, T.; Sakuma, H.; Takenoshita, S.; Omata, S.; Constantinou, C. E. Development of a New Instrument for Examination of Stiffness in the Breast Using Haptic Sensor Technology. *Sens. Actuators, A* **2008**, *143*, 430−438.

(35) Ayyildiz, M.; Guclu, B.; Yildiz, M. Z.; Basdogan, C. An Optoelectromechanical Tactile Sensor for Detection of Breast Lumps. *IEEE Trans. Haptics* **2013**, *6*, 145−155.

(36) Rangayyan, R. M.; Mudigonda, N. R.; Desautels, J. E. L. Boundary Modeling and Shape Analysis Methods for Classification of Mammographic Masses. *Med. Biol. Eng. Comput.* **2000**, *38*, 487−496.

(37) Friedman, R. J.; Rigel, D. S.; Kopf, A. W. Early Detection of Malignant-Melanoma - the Role of Physician Examination and Self-Examination of the Skin. *Ca-Cancer J. Clin.* **1985**, *35*, 130−151.

(38) Nguyen, C.; Maheshwari, V.; Saraf, R. F. Ultrasoft 100 nm Thick Zero Poisson's Ratio Film with 60% Reversible Compressibility. *Nano Lett.* **2012**, *12*, 2171−2175.

(39) Maheshwari, V.; Saraf, R. Tactile Devices to Sense Touch on a Par with a Human Finger. *Angew. Chem.* **2008**, *47*, 7808−7826.

(40) Schwartz, G.; Tee, B. C. K.; Mei, J. G.; Appleton, A. L.; Kim, D. H.; Wang, H. L.; Bao, Z. N. Flexible Polymer Transistors with High Pressure Sensitivity for Application in Electronic Skin and Health Monitoring. *Nat. Commun.* **2013**, *4*, 1859.